Singular Extremals for the Time-Optimal Control of Dissipative Spin $\frac{1}{2}$ Particles

M. Lapert,[1] Y. Zhang,[2] M. Braun,[2] S. J. Glaser,[2] and D. Sugny[1,*]

[1]*Laboratoire Interdisciplinaire Carnot de Bourgogne (ICB), UMR 5209 CNRS-Université de Bourgogne,*
9 Avenue A. Savary, BP 47 870, F-21078 DIJON Cedex, France
[2]*Department of Chemistry, Technische Universität München, Lichtenbergstrasse 4, D-85747 Garching, Germany*
(Received 6 November 2009; published 24 February 2010)

We consider the time-optimal control by magnetic fields of a spin $\frac{1}{2}$ particle in a dissipative environment. This system is used as an illustrative example to show the role of singular extremals in the control of quantum systems. We analyze a simple case where the control law is explicitly determined. We experimentally implement the optimal control using techniques of nuclear magnetic resonance. To our knowledge, this is the first experimental demonstration of singular extremals in quantum systems with bounded control amplitudes.

Optimal control theory can be viewed as a generalization of the classical calculus of variations for problems with dynamical constraints. Its modern version was born with the Pontryagin maximum principle (PMP) in the late 1950s [1]. Its development was originally inspired by problems of space dynamics, but it is now a key tool to study a large spectrum of applications such as robotics, economics, and quantum mechanics. Solving an optimal control problem means finding a particular control law, the optimal control, such that the corresponding trajectory satisfies given boundary conditions and minimizes a cost criterion. Examples of cost functionals of physical interests are the energy and the duration of the control. A strategy for solving an optimal control problem consists in finding extremal trajectories which are solutions of a generalized Hamiltonian system subject to the maximization condition of the PMP. In a second step, one selects among the extremals the ones which effectively minimize the cost criterion. Although its implementation looks straightforward, the practical use of the PMP is far from being trivial and each control has to be analyzed using geometric and numerical methods. The first applications of optimal control theory in quantum dynamics began in the mid 1980s [2]. Continuous advances have been done both theoretically and experimentally [3]. Among the set of extremal trajectories determined from the PMP, one distinguishes regular and singular ones (see below for a concrete definition). Surprisingly, whereas regular extremals are well known, the existence and the potential applications of singular extremals in quantum control have been largely ignored in the chemical-physics literature and only few results exist [4–9]. Note that the zero field used in the optimal control of quantum systems with unbounded control [8,10] can be viewed as a limit case of singular extremals when the maximum amplitude of the control goes to infinity (see [6] for details). In this Letter, we consider a simple physical example, a spin $\frac{1}{2}$ particle in a dissipative environment, which highlights the crucial role of singular controls. For instance, a gain of almost 60% in

the control duration can be obtained over the standard inversion recovery sequence when using singular extremals (see Fig. 1). We take advantage of this example to explain the mathematical framework and to detail in the last section its physical interpretation. The optimal control law is also implemented experimentally using techniques of nuclear magnetic resonance (NMR).

In the considered case of resonant radiation, the state of the system can be completely represented by a two-dimensional state vector $X \in \mathbb{R}^2$ and a single control u is sufficient [4]. The corresponding controlled system is de-
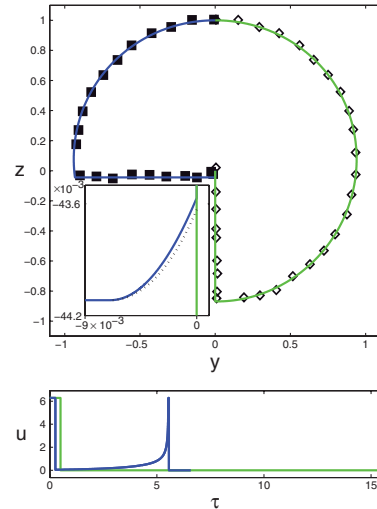

FIG. 1 (color online). Plot of the optimal trajectories (blue or dark gray curve) and of the inversion recovery sequence (green or gray curve) in the plane (y, z) for $T_1 = 740$ ms, $T_2 = 60$ ms and $\omega_{\max}/(2\pi) = 32.3$ Hz. The experimentally measured trajectories are represented by filled squares and open diamonds, respectively. The corresponding control laws are represented in the lower panel. In the upper panel, the small insert represents a zoom of the optimal trajectory near the origin. The dotted line is the switching curve originating from the horizontal singular line. The vertical green line corresponds to the intuitive solution. The solid blue curve is the optimal trajectory near the origin.

fined by differential equations of the form $\dot{X} = F_0(X) + uF_1(X)$ and the control parameter satisfies $|u| \leq u_0$, which defines the set of admissible controls. The objective of the control is to determine a function $u(t)$ such that the system goes in minimum time from the initial point X_0 to a target state X_1. We use for that the PMP which can be sketched as follows [1,11,12]. We introduce the pseudo-Hamiltonian $\mathcal{H}(X, P, u) = P(F_0 + uF_1)$ where the adjoint state $P \in \mathbb{R}^{*2}$ for any time t. An optimal trajectory is solution of the equations

$$\dot{X}(t) = \frac{\partial \mathcal{H}}{\partial P}, \qquad \dot{P}(t) = -\frac{\partial \mathcal{H}}{\partial X},$$

where u is obtained from the maximization condition $\mathcal{H}(X, P, u) = H(X, P) = \max_{v \in [-u_0, u_0]}[\mathcal{H}(X, P, v)]$ with the condition $H(X, P) \geq 0$ [12]. For controlled systems on the coordinate plane $\mathbb{R}^2$, the solutions of the PMP take a very simple form. We consider the switching function $\phi(X, P) = PF_1$ [12], which is the only term of $\mathcal{H}$ on which the control can act. When $\phi(X, P) \neq 0$, one immediately sees that the maximization condition leads to bang controls, i.e., to controls of constant and maximum amplitude of the form $u = u_0 \, \text{sgn}[\phi] = \pm u_0$. These extremals are the regular ones. If ϕ vanishes in an isolated point then the control field switches from $\pm u_0$ to $\mp u_0$. The singular situation is encountered when the switching function vanishes on a given time interval. In this case, the control cannot be directly determined by the maximization condition. The control parameter is instead computed by requiring that $\phi(X, P) = 0$ on the singular arc, which leads to the relations $\phi(X, P) = \dot{\phi}(X, P) = \ddot{\phi}(X, P) = \cdots = 0$. This condition allows us to identify the manifolds, here lines of the coordinate plane on which the singular trajectory lies. Note also that in this case, the control field is not constantly equal to $+u_0$ or $-u_0$, but belongs to the interval $[-u_0, u_0]$. The final optimal control law is determined by gluing together singular and regular arcs.

One of the most promising fields of applications of quantum control is the control of spin systems in NMR [13]. We use such systems in this Letter to show the role of singular extremals in the time-optimal control of quantum dynamics. In a first step, we consider a spin $\frac{1}{2}$ particle in a dissipative environment whose dynamics is governed by the Bloch equation:

$$\begin{pmatrix} \dot{M}_x \\ \dot{M}_y \\ \dot{M}_z \end{pmatrix} = \begin{pmatrix} -M_x/T_2 \\ -M_y/T_2 \\ +(M_0 - M_z)/T_1 \end{pmatrix} + \begin{pmatrix} \omega_y M_z \\ -\omega_x M_z \\ \omega_x M_y - \omega_y M_x \end{pmatrix},$$

where $\vec{M}$ is the magnetization vector and $\vec{M}_0 = M_0 \vec{e}_z$ is the equilibrium point of the dynamics. We assume that the control field $\vec{\omega} = (\omega_x, \omega_y, 0)$ satisfies the constraint $|\vec{\omega}| \leq \omega_{max}$. We introduce the normalized coordinates $\vec{x} = (x, y, z) = \vec{M}/M_0$, which entails that at thermal equilibrium the z component of the scaled vector $\vec{x}$ is by definition $+1$. The normalized control field which satisfies $|u| \leq 2\pi$

is defined as $u = (u_x, u_y, 0) = 2\pi\vec{\omega}/\omega_{max}$, while the normalized time τ is given by $\tau = (\omega_{max}/2\pi)t$. Dividing the previous system by $\omega_{max} M_0/(2\pi)$, one deduces that the dynamics of the normalized coordinates is ruled by the following system of differential equations:

$$\begin{pmatrix} \dot{x} \\ \dot{y} \\ \dot{z} \end{pmatrix} = \begin{pmatrix} -\Gamma x \\ -\Gamma y \\ \gamma - \gamma z \end{pmatrix} + \begin{pmatrix} u_y z \\ -u_x z \\ u_x y - u_y x \end{pmatrix},$$

where $\Gamma = 2\pi/(\omega_{max} T_2)$ and $\gamma = 2\pi/(\omega_{max} T_1)$.

We consider the control problem of bringing the system from the equilibrium point $\vec{M}_0$ to the zero-magnetization point which is the center of the Bloch ball. In the setting of NMR spectroscopy and imaging, this corresponds to saturating the signal, e.g., for solvent suppression or contrast enhancement, respectively [14]. Since the initial point belongs to the z axis, it can be shown that the controlled system is equivalent to a system with only one control where, e.g., $u_y = 0$ [4]. Roughly speaking, this means that the meridian planes of the Bloch sphere play all the same role for the optimal trajectory. Taking $u_y = 0$, we are thus considering a problem in a plane of the form:

$$\begin{pmatrix} \dot{y} \\ \dot{z} \end{pmatrix} = \begin{pmatrix} -\Gamma y \\ \gamma - \gamma z \end{pmatrix} + u \begin{pmatrix} -z \\ y \end{pmatrix}$$

where the subscript x has been omitted for the control parameter. We can then apply for this system the theoretical description of the previous paragraph where $F_0 = (-\Gamma y, \gamma - \gamma z)$ and $F_1 = (-z, y)$.

As detailed above, we introduce the switching function $\phi = PF_1 = -p_y z + p_z y$ [12]. Using the fact that $\frac{d\phi}{dt} = PV$ where $V = (-\gamma + \gamma z - \Gamma z, -\Gamma y + \gamma y)$ and the relations $PF_1 = PV = 0$ on a singular arc, one deduces that the vectors F_1 and V must be parallel on this set since P is non zero. This means that the singular trajectories belong to the set $S = \{X \in \mathbb{R}^2 | \det(F_1, V) = 0\}$ which corresponds to the union of the vertical line $y = 0$ and of the horizontal one with z given by

$$z_0 = -\frac{\gamma}{2(\Gamma - \gamma)} = -\frac{T_2}{2(T_1 - T_2)}$$

if $\Gamma \neq \gamma$ (or equivalently if $T_1 \neq T_2$). The corresponding singular control u_s, which is determined from the condition $\dot{\phi}(X, P) = 0$, is given by

$$u_s(y, z) = \frac{-y\gamma(\Gamma - 2\gamma) - 2yz_0(\gamma^2 - \Gamma^2)}{2(\Gamma - \gamma)(y^2 - z_0^2) - \gamma z_0}. \qquad (1)$$

Note that the control u_s is not defined as a function of the time but as a function of y and z. One also deduces that this singular control vanishes on the vertical singular line and that it is admissible, i.e., $|u_s| \leq 2\pi$, on the horizontal one if $|y| \geq |\gamma(\gamma - 2\Gamma)|/[2\pi(2\Gamma - 2\gamma)]$. For smaller values of y, the system cannot follow the horizontal singular arc and a switching curve appears from the point where the admissibility is lost [12]. A switching curve is a line in the plane

(y, z) where the optimal control changes sign when crossing it.

The optimality of the singular trajectories can be determined geometrically by introducing the clock form α which is a 1 form such that $\alpha(F_0) = 1$ and $\alpha(F_1) = 0$. The form α is defined on points where F_0 and F_1 are not collinear. Let γ_1 and γ_2 be two extremals starting and ending at the same points and τ_1 and τ_2 the corresponding times needed to follow the two trajectories. The clock form allows us to determine the time taken to travel a path since, for instance, $\int_{\gamma_1} \alpha = \int_0^{\tau_1} \alpha(\dot{X}) d\tau = \int_0^{\tau_1} \alpha(F_0) d\tau = \tau_1$. To compare τ_1 and τ_2, we consider the loop $\gamma_1 \bigcup \gamma_2^{-1}$ where γ_2^{-1} is γ_2 run backward. Introducing the surface D delimited by γ_1 and γ_2, a simple computation leads to $\int_{\gamma_1 \bigcup \gamma_2^{-1}} \alpha = \int_D d\alpha$. Since $d\alpha$ is equal to zero only on the singular set and remains of constant sign outside [11], one obtains that $\tau_1 - \tau_2 = \int_D d\alpha$. In particular, it can be shown that the horizontal singular line is locally optimal and that the vertical one is optimal if $z > z_0$.

The control problem used for illustration is defined by the relaxation parameters γ^{-1} and Γ^{-1} (expressed in the normalized time unit defined above) of 23.9 and 1.94, respectively. We compare the optimal control law with an intuitive one used in NMR. The intuitive solution, the so-called inversion recovery (IR) sequence [14], is composed of a bang pulse to reach the opposite point of the initial state along the z axis followed by a zero control where we let the dissipation act up to the center of the Bloch ball. The optimal and the IR solutions are plotted in Fig. 1. Geometric tools allow us to show that the optimal control is the concatenation of a bang pulse, followed successively by a singular control along the horizontal singular line, another bang pulse and a zero singular control along the vertical singular line. Figure 1 displays also the switching curve which has been determined numerically by considering a series of trajectories with $u = +2\pi$ originating from the horizontal singular set where $\phi = 0$. The points of the switching curve correspond to the first point of each trajectory where the switching function vanishes. We have also checked that the second bang pulse of the optimal sequence does not cross the switching curve up to the vertical singular axis. In this example, a gain of 58% is obtained for the optimal solution over the intuitive one, which clearly shows the importance of singular extremals.

Both pulse sequences were implemented experimentally on a Bruker Avance 250 MHz spectrometer with linearized amplifiers. The experiments were performed using the proton spins of H_2O. The sample consists of 10% H_2O, 45% D_2O, and 45% deuterated glycerol, saturated with $CuSO_4$. At room temperature (298 K) the relaxation times were $T_1 = 740$ ms, $T_2 = 60$ ms, which correspond to the unitless values given above for $\omega_{max}/(2\pi) = 32.3$ Hz. For this value of ω_{max}, the duration of the intuitive IR sequence is 478 ms, whereas the optimal sequence has a duration of only 202 ms. The experimentally measured trajectories of the Bloch vector are also shown in Fig. 1 for the optimal

sequence (filled squares) and the IR sequence (open diamonds). The reasonable match between theory and experiment confirms that the complex pulse sequence required for optimization can really be implemented with modern NMR spectrometers.

Figure 2 displays the evolution of the optimal solution and of the intuitive one when the maximum amplitude of the control field varies. The ratio between the two control durations T_{opt} and T_{IR} is also plotted as a function of $\omega_{max}/2\pi$. For low values of ω_{max}, the optimal pulse and the IR sequence are very similar and the ratio is close to 1. Note that for $\omega_{max}/2\pi \lesssim 2.7$, the target state cannot be reached from the initial point so the ratio cannot be defined. We observe a rapid decrease of this ratio when ω_{max} increases showing the crucial role of the horizontal singular line. The gain tends asymptotically to a constant value when $\omega_{max} \rightarrow +\infty$ for fixed values of T_1 and T_2. In this limit, we can neglect the duration of the different bang controls. Using the relation $\omega_s = \frac{\omega_{max}}{2\pi} u_s = \frac{T_2 - 2T_1}{2T_1(T_1 - T_2)y}$, one obtains by a direct integration of the Bloch equation that

$$T_{opt} \underset{\omega_{max} \rightarrow +\infty}{\rightarrow} \frac{T_2}{2} \log\left(1 - \frac{2}{\alpha T_2}\right) + T_1 \log\left(\frac{2T_1 - T_2}{2(T_1 - T_2)}\right),$$

$$T_{IR} \underset{\omega_{max} \rightarrow +\infty}{\rightarrow} T_1 \log 2,$$

where $\alpha = \frac{T_2(T_2 - 2T_1)}{2T_1(T_1 - T_2)^2}$, which leads to a limit ratio of 0.389.

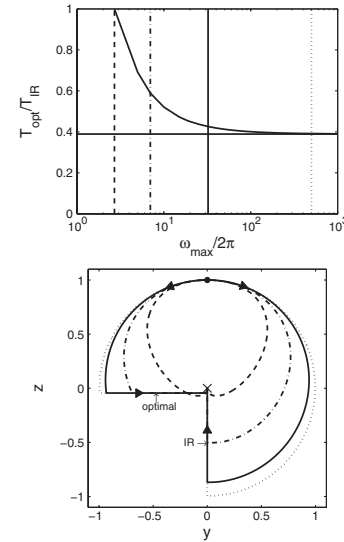
FIG. 2.   (top) Ratio T_{opt}/T_{IR} as a function of $\omega_{max}/(2\pi)$. The horizontal line indicates the position of the limit ratio when $\omega_{max} \rightarrow +\infty$. (bottom) Optimal trajectories (left part) and the inversion recovery sequences (right part) for four values of $\omega_{max}/(2\pi)$, 2.7, 7, 32.3, and 500 Hz. The vertical lines of the top panel correspond to the four solutions of the bottom panel. The solid curve is the case considered in Fig. 1. The black dot and the cross represent, respectively, the positions of the initial and final points. The small arrows indicate the way the trajectories are followed.
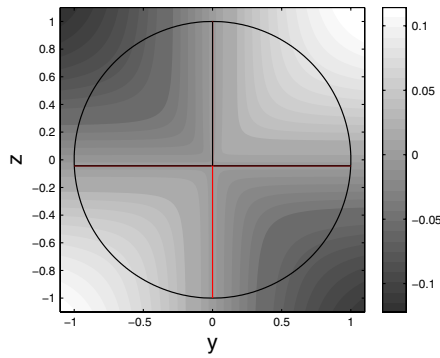
FIG. 3 (color online). Contour plot of the function $d\dot{r}/d\theta$ as a function of y and z. The solid lines represent the set of zeros of $d\dot{r}/d\theta$ or the singular set S (see the text). The time-minimum and time-maximum singular lines are plotted, respectively, in black and red (light gray). The circle is the projection of the Bloch sphere in the plane (y, z).

Physical interpretation of the optimal control strategy.— In the example considered, the role of singular extremals can be physically interpreted in light of the dissipation effects. We introduce the polar coordinates (r, θ) such as $y = r\cos\theta$ and $z = r\sin\theta$. A straightforward computation then leads to

$$\dot{r} = -(\Gamma\cos^2\theta + \gamma\sin^2\theta)r + \gamma\sin\theta,$$

$$d\dot{r}/d\theta = -(\gamma - \Gamma)r\sin(2\theta) + \gamma\cos\theta$$

(see Fig. 3). One immediately sees that the control field u cannot modify the radial velocity but only the orthoradial one $\dot{\theta}$. To reach in minimum time the center of the Bloch ball, the idea is then at each time to be on the point where $|\dot{r}|$ is maximum for a fixed value of the radial coordinate r. The singular control u_s defined in Eq. (1) is determined so that the dynamics stays on the line of maximum variation of the radius r. In other words, this means that the set of solutions of the equation $d\dot{r}/d\theta = 0$ is exactly the set S. One deduces that the strategy of the optimal control can be thought of as follows. A first bang pulse is applied to the system to reach the horizontal singular line. The radius r is then optimally reduced along this curve as long as the control field satisfies the constraint of the control problem. The local optimality of this line can be recovered by showing that the points of this set are associated to maxima of the function $|\dot{r}|(r, \theta)$ for r fixed. When the limit of admissibility is attained, a new bang pulse is applied to reach the vertical singular line in a region where this set is optimal. We finally arrive to the target state along this curve. We recover here a mechanism introduced in [10] for cooling a two-level system.

Conclusion and prospective views.—We hope that this example of singular extremals in the control of a spin $\frac{1}{2}$ particle in a dissipative environment will motivate systematic investigations of singular controls in quantum mechan-

ics. The question of the role of singular extremals in more complicated systems or in quantum computing remains completely open. The next step of this study could be the analysis of the optimal control of coupled spins with bounded fields generalizing thus the different works in this domain with unbounded controls [8].

*dominique.sugny@u-bourgogne.fr

[1] L. S. Pontryagin *et al.*, *The Mathematical Theory of Optimal Processes* (John Wiley and Sons, New York, London, 1962).

[2] S. Conolly, D. Nishimura, and A. Macovski, IEEE Trans. Med. Imaging **5**, 106 (1986).

[3] S. Rice and M. Zhao, *Optimal Control of Quantum Dynamics* (Wiley, New York, 2000); M. Shapiro and P. Brumer, *Principles of Quantum Control of Molecular Processes* (Wiley, New York, 2003).

[4] B. Bonnard and D. Sugny, SIAM J. Control Optim. **48**, 1289 (2009); B. Bonnard, M. Chyba, and D. Sugny, IEEE Trans. Autom. Control **54**, 2598 (2009); D. Sugny, C. Kontz, and H. R. Jauslin, Phys. Rev. A **76**, 023419 (2007); D. Sugny and C. Kontz, Phys. Rev. A **77**, 063420 (2008).

[5] U. Boscain and G. Charlot, ESAIM Control Optim. Calc. Var. **10**, 593 (2004).

[6] U. Boscain and P. Mason, J. Math. Phys. (N.Y.) **47**, 062101 (2006).

[7] D. D'Alessandro, IEEE Trans. Autom. Control **46**, 866 (2001).

[8] N. Khaneja, R. Brockett, and S. J. Glaser, Phys. Rev. A **63**, 032308 (2001); N. Khaneja, S. J. Glaser, and R. Brockett, Phys. Rev. A **65**, 032301 (2002); N. Khaneja, T. Reiss, B. Luy, and S. J. Glaser, J. Magn. Reson. **162**, 311 (2003); N. Khaneja, B. Luy, and S. J. Glaser, Proc. Natl. Acad. Sci. U.S.A. **100**, 13 162 (2003).

[9] R. Wu, J. Dominy, T.-S. Ho, and H. Rabitz, arXiv:0907.2354v1 [J. Math. Phys. (to be published)].

[10] S. E. Sklarz, D. J. Tannor, and N. Khaneja, Phys. Rev. A **69**, 053408 (2004); D. J. Tannor and A. Bartana, J. Phys. Chem. A **103**, 10359 (1999).

[11] B. Bonnard and M. Chyba, *Singular Trajectories and their Role in Control Theory*, Mathématiques and Applications Vol. 40 (Springer-Verlag, Berlin, 2003).

[12] U. Boscain and B. Piccoli, *Optimal Syntheses for Control Systems on 2-D Manifolds*, Mathématiques and Applications Vol. 43 (Springer-Verlag, Berlin, 2004).

[13] M. H. Levitt, *Spin Dynamics: Basics of Nuclear Magnetic Resonance* (John Wiley and Sons, New York, London, Sydney, 2008).

[14] S. L. Patt and B. D. Sykes, J. Chem. Phys. **56**, 3182 (1972); G. M. Bydder, J. V. Hajnal, and I. R. Young, Clinical Radiology **53**, 159 (1998).